SCIENTIFIC Publishing Limited

Electrical Engineering and Technology

https://ojs.ukscip.com/index.php/eet

Article

Power Management in Hybrid PV-Wind-Battery Microgrids for Enhanced Efficiency

Muhammad Qasim Nawaz , Muhammad Saqib Niaz * and Usman Muhammad

College of Electrical, Energy and Power Engineering, Yangzhou University, Yangzhou 225000, China

* Correspondence: mh24188@stu.yzu.edu.cn

Received: 8 September 2025; **Revised:** 6 November 2025; **Accepted:** 11 November 2025; **Published:** 3 December 2025

Abstract: As the penetration of renewable energy soars in power systems, engineers are continuously seeking better ways to improve the efficiencies of renewable energy conversion systems. This study investigates a MATLAB (matrix laboratory)-based control strategy for power management in a hybrid direct current (DC) microgrid incorporating photovoltaic (PV) panels, wind turbines, and battery storage. The objective is to enhance the stability and efficiency of energy distribution through advanced power control techniques. A simulation-driven methodology was employed to assess the performance of various control strategies, including Maximum Power Point Tracking (MPPT) and battery management algorithms, under dynamic environmental conditions. Key findings show that PV voltage fluctuates between 200 V and 300 V, with power outputs ranging from 500 W to 1,200 W, highlighting the system's adaptability to changes in irradiance. The battery system maintains voltage stability at 250 V with current fluctuations within ±5 A, ensuring effective load balancing. The integration of PV, wind, and battery systems optimizes power synchronization, with PV power ranging from 1,000 W to 2,000 W, wind power stabilizing around 3,000 W, and battery power oscillating between −2,000 W and 1,000 W. The results demonstrate that advanced control algorithms significantly reduce power fluctuations, ensuring stable microgrid operation and facilitating the integration of renewable energy sources for decentralized and off-grid applications. These findings underscore the potential for improving energy efficiency and supporting sustainable energy infrastructure development.

Keywords: Power Management; Renewable Energy Integration; DC Microgrid Optimization; Maximum Power Point Tracking; Battery Energy Storage

1. Introduction

The growing emphasis on sustainable energy integration has increased the adoption of hybrid renewable energy systems, particularly those combining photovoltaic (PV) panels, wind turbines (WTs), and battery storage systems within DC microgrids [1]. These microgrids offer promising pathways for enhancing energy density, reliability, and power quality, which are crucial for meeting dynamic energy demands [2]. However, effective power management in DC microgrids remains challenging, particularly in optimizing power flow, ensuring stability, and addressing the intermittency of renewable sources [3,4]. Current approaches often lack the robustness required to respond dynamically to fluctuating load demands and renewable generation, a critical gap that underscores the necessity of this research [5,6].

The cumulative growth in hybrid renewable systems, encompassing photovoltaic (PV), wind, and battery storage capacities from 2000 to 2024, is illustrated in **Figure 1**. The red bars represent the annual wind energy capacity additions, which begin at approximately 5 GW in 2000 and expand significantly to around 230 GW by 2024, high-

lighting the rapid advancement of wind power [7, 8]. The blue bars indicate the cumulative addition of solar PV capacity, starting from 0.5 GW in 2000 and progressively increasing to an estimated 55 GW by 2024, underscoring the growing role of solar energy in hybrid systems. Battery storage, shown in green, reflects a more modest initial growth, with capacity rising from a minimal 0.2 GW in 2000 to 28 GW in 2024. Collectively, these metrics demonstrate a steady and substantial expansion in hybrid renewable energy systems, driven by technological advancements and increased demand for sustainable power solutions. Despite notable advancements, existing literature does not comprehensively address the complexities of hybrid power management, especially within decentralized systems. For instance, recent studies emphasize technical frameworks yet overlook implementation challenges specific to hybrid PV-wind-battery microgrids [9]. Furthermore, the need for enhanced control strategies that can autonomously stabilize power flow in fluctuating conditions remains largely unmet [10]. Prior research utilizing MATLAB has demonstrated potential for modeling and managing renewable energy dynamics; however, significant gaps in ensuring resilient, efficient, and cost-effective energy distribution persist [11].

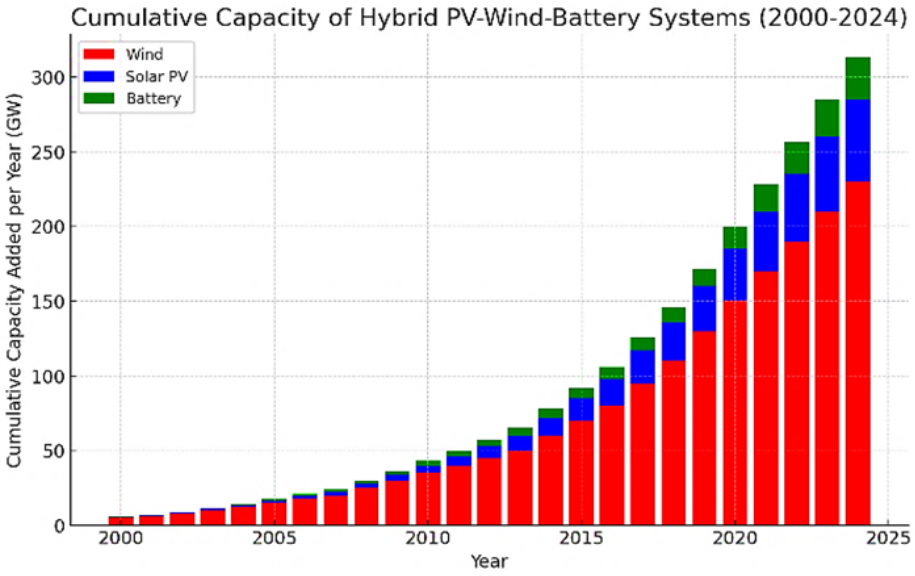

Figure 1. Net installed capacity addition wise trends of wind, solar, and battery (2000–2024) [7,8].

In response to these gaps, this study offers a novel approach using MATLAB to advance power management by simulating real-world scenarios and assessing robust strategies for optimizing efficiency and stability in hybrid microgrids. The objectives of this research are threefold: to address stability and load balance in DC microgrids, improve fault tolerance for isolated or low-growth regions, and promote renewable energy adoption through an adaptable control framework. By filling critical gaps in existing methodologies, this study contributes a unique perspective to the growing body of work on decentralized renewable energy solutions. This approach enhances power control capabilities while proactively contributing to cost management and the optimal utilization of energy resources. Moreover, designing fault-tolerant energy systems is essential, particularly for standalone or low-growth regions where conventional power infrastructure is limited or unreliable [12]. This study aims to advance the use of MATLAB in achieving grid stability and to foster the integration of renewable energy within decentralized power systems, addressing the unique challenges faced by such infrastructures. Through dynamic simulations and tailored control strategies, the research seeks to support sustainable, resilient energy solutions for decentralized applications.

2. Literature Review

This literature review analyzes advancements and challenges in optimizing power management for DC microgrids with hybrid renewable energy systems (HRES) from 2020 to 2024 [1,10]. The review focuses on integrating photovoltaic panels, WTs, and battery storage to enhance energy stability, flexibility, and economic viability. Key

challenges remain in adapting control models for high-demand scenarios, improving cost-effectiveness in decentralized areas, and using real-time analytics to manage variable renewable inputs [3]. Findings highlight improvements in battery lifespan, renewable reliance, and social electrification, but emphasize the need for scalable, adaptive solutions for diverse operational settings. **Table 1** provides a comparative evaluation of current methods, outlining essential research priorities for sustainable DC microgrid operations with HRES.

Table 1. Literature Review on Power Management Strategies for DC Microgrids with HRES.

Related Study	Research Approach	Identification of Gaps	Key Findings
Halmous et al. [13]	Energy sharing with supercapacitors	Lacks robustness during high-demand scenarios and renewable intermittency	Improved power flexibility by approximately 20% in testing but limited during peak loads, indicating potential for 10–15% further stabilization with predictive analytics
Thango and Obokoh [14]	Techno-green HRES cost analysis	Limited application to off-grid rural areas	Achieved 25–30% reduction in energy expenses in urban settings, but applicability in rural areas remains untested
Hosny et al. [15], Premadasa et al. [16]	Multi-objective PV-wind-battery model	Does not address diverse climate operational complexities	Optimized renewable energy use, achieving up to 45% reliance on renewables in urban test cases
Abd-El Baset et al. [17], Khallouf et al. [18]	Fuzzy optimization for power flow	Lacks real-time adaptive features for load variation management	Enhanced energy stability by 18% under controlled load conditions, suggesting potential improvements with adaptive controls
Premadasa et al. [16], Jasim et al. [19]	Size optimization for zero-carbon	Limited focus on economic feasibility for broader adoption	Environmentally beneficial, reducing carbon emissions by up to 40%, but broader adoption is hindered by high initial setup costs
Mhandu and Longe [20]	Techno-economic hybrid PV-wind-diesel	Primarily applicable to diesel-supplemented systems	Demonstrated economic viability, reducing costs by 15–20% in hybrid PV-wind-diesel setups
Kandari et al. [9], Panda et al [21]	Battery efficiency in PV-wind systems	Neglects alternative energy storage integrations	Improved cost-performance by increasing battery lifespan by 10%, focusing solely on battery efficiency
Premadasa et al. [16], Rico-Riveros et al. [22]	Off-grid PV-wind system reliability	Missing energy efficiency metrics critical for sustainability	Increased reliability by 20% using Loss-of-Load Probability, but lacks focus on efficiency metrics for sustainable use
Rico-Riveros et al. [22]	Hybrid solar-biomass for electrification	Lacks a dynamic control model for adapting to fluctuating renewable input	Addressed social electrification needs, achieving 85% power availability in pilot studies without dynamic controls
Tighirt et al. [3], Saimadhuri and Janaki [6], Singh and Lather [11]	Advanced control in DC microgrids	Need for real-time communication and decision-making strategies	Emphasized adaptive control, improving response time by 25% for load variations
Ayele et al. [23], Murugan and Vijayarajan [24]	Secure communication in microgrids	Insufficient focus on smart decision-making protocols for optimized power flow	Highlighted secure communication, achieving a 95% reliability rate in secure data transmission within the DC microgrid
Tang et al. [25], Peres et al. [26]	Load-shedding for wind power fluctuation	Lacks detailed energy coordination framework	Improved stability by 30% through load-shedding under fluctuating wind conditions
Zarma et al. [27]	Machine learning for energy prediction	Missing a framework for real-time integration of predictive analytics in microgrid operations	Advanced power prediction, achieving 92% accuracy in power demand forecasting using machine learning

Contribution of This Research

This research on power management in hybrid PV-Wind-Battery microgrids contributes to addressing energy challenges by improving renewable energy reliability in isolated and off-grid areas. By optimizing energy distribution across photovoltaic, wind, and battery sources, it supports efficient, adaptable, and sustainable power systems that respond to variable demand. Additionally, the study advances DC microgrid technology through innovative control strategies that enhance renewable energy utilization and storage management, promoting technological growth and practical applications in remote regions.

3. System Design and Components

The design of the power management system for hybrid PV-Wind-Battery microgrids, illustrated in **Figure 2**, enables efficient power supply management through the integration of renewable energy sources, specifically photovoltaic (PV) panels and WTs, in conjunction with battery storage. This system dynamically regulates the operation of PV panels and WTs, balancing energy output by diverting excess power to battery storage or supplying it directly to the load, depending on real-time demand. During periods of low renewable energy production, the bat-

teries supply power, thereby enhancing the overall system efficiency. This design enables adaptive management of supply and demand, minimizing energy waste and ensuring a reliable, responsive energy provision.

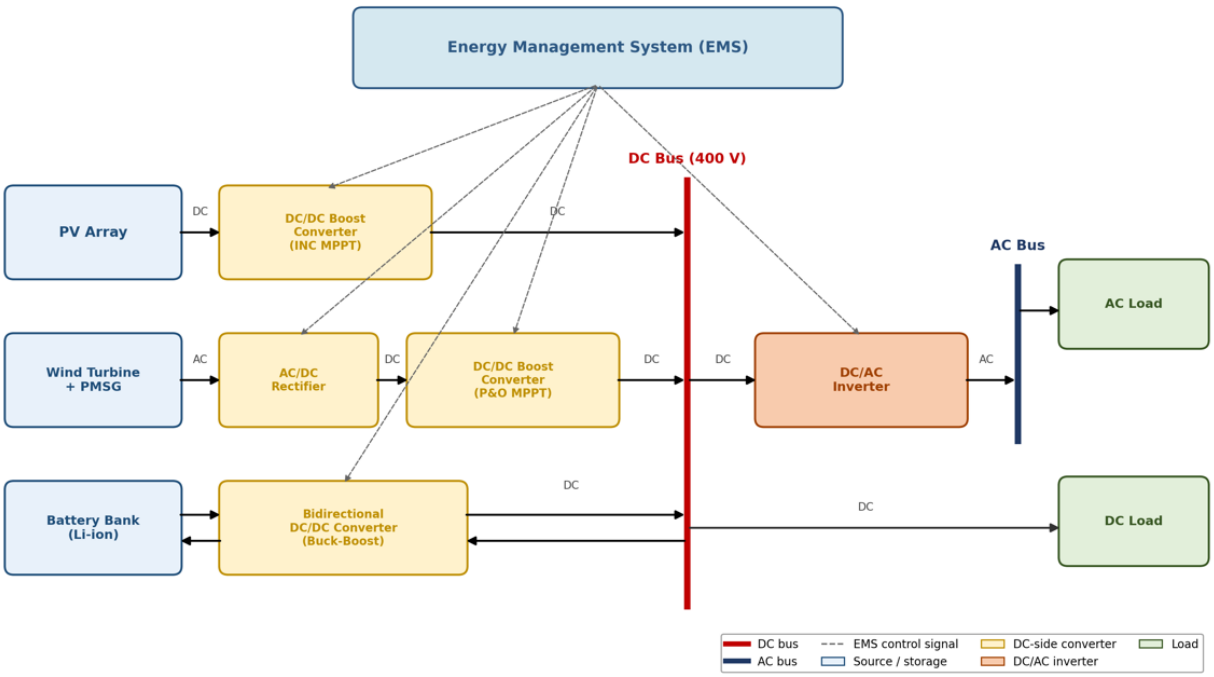

Figure 2. Block diagram for Hybrid PV-Wind-Battery DC microgrid showing dedicated power electronic converters between each source/storage and common DC bus.

The system's control strategies maximize renewable energy use and minimize reliance on non-renewables, providing sustainable power for off-grid areas. Designed for both grid-connected and standalone modes, it offers flexibility across applications. Key elements, including inverters and energy management systems (EMS), regulate voltage, stabilize frequency, and balance loads. An integrated algorithm forecasts energy demand and generation, optimizing resource use to maintain stable supply and reduce carbon emissions.

3.1. DC Microgrid Architecture

The proposed DC microgrid architecture connects each source and storage unit to the common DC bus through its corresponding power electronic converter. The PV array is connected through a DC-DC boost converter controlled by the Incremental Conductance (INC) MPPT algorithm. The wind turbine/Permanent Magnet Synchronous Generator (PMSG) unit is connected through a three-phase rectifier followed by a DC-DC boost converter controlled by the Perturb and Observe (P&O) MPPT algorithm. The battery bank is interfaced through a bidirectional DC-DC converter to support both charging and discharging. These converters feed a regulated 400 V DC bus, which supplies the DC load directly and can also supply alternating current (AC) loads through an inverter.

3.2. Energy Storage Systems

EMS is one of the central components of the hybrid PV-Wind-Battery microgrids for renewable energy management and power grid stability. These systems are batteries that capture additional energy produced by PV panels and WTs during the optimum conditions in order to maintain consistency and provide energy during low generation periods. Batteries have become the preferred form of Energy Storage Systems (ESSs) in such microgrids because they regulate supply and demand, lessen fossil fuel dependence, and absorb fluctuations in the grid. In more complex hybrid systems, it is the intelligent management of the stored energy where the efficiency and effectiveness are outdone in terms of use of available power and less environmental impact in off-grid or remote locations.

3.3. Control Algorithms for Power Management

To illustrate the power management process in a Hybrid PV-Wind-Battery microgrid, the flowchart in **Figure 3** provides a step-by-step overview. The process begins with assessing solar PV and wind power outputs along with the load demand. If the grid is accessible, the microgrid operates in grid-connected mode. When the combined PV and wind power exceed demand, the surplus is fed back to the grid; conversely, if they fall short, additional power is drawn from the grid. If grid access is unavailable, the system switches to off-grid mode. Next, when PV and wind power exceed the load, the system checks the battery's State of Charge (SOC). If the SOC is below its maximum threshold, the surplus charges the battery. When the battery is fully charged, PV and wind output are curtailed to prevent over-generation. If the SOC falls below its minimum, the battery discharges to meet the load. Should generation still be insufficient, load shedding is employed to balance supply with demand.

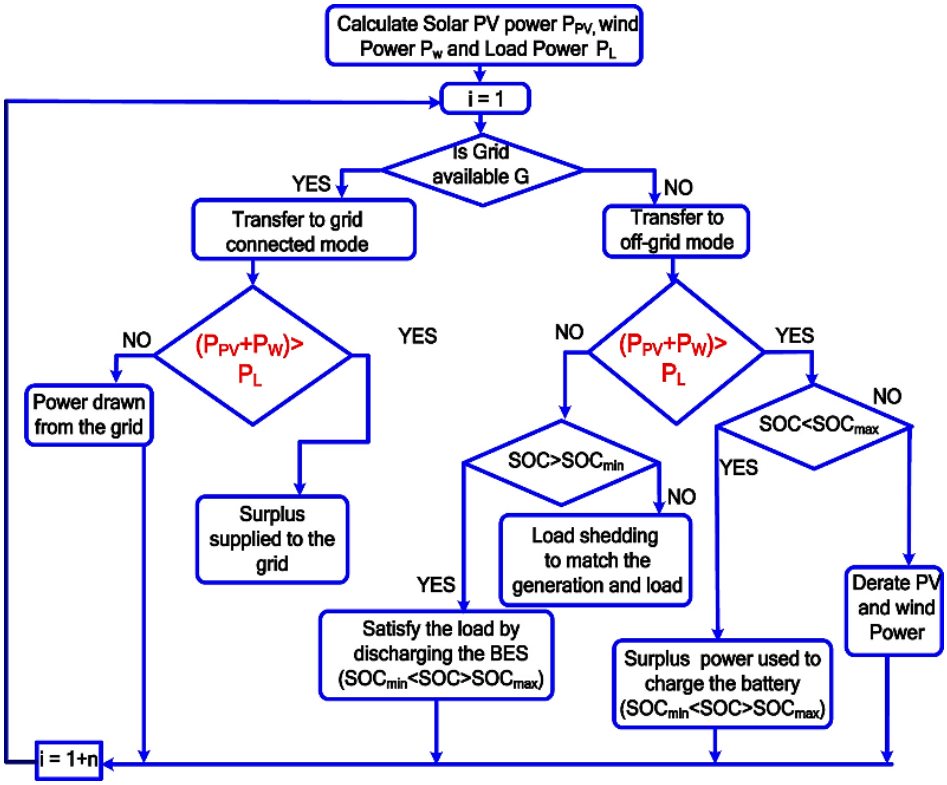

Figure 3. Power management flowchart for the hybrid PV-wind-battery DC microgrid under grid-connected and islanded operating modes.

4. Modeling Renewable Energy Sources

The effective deployment of renewable energy sources, such as wind, solar, and battery storage, requires accurate modeling of each component to maximize power output. WTs are represented using fluid dynamics and mechanical equations to assess conversion efficiency, accounting for wake effects and site-specific characteristics. Solar panels are modeled using a photovoltaic (PV) electrical framework, estimating electricity production based on irradiance and temperature conditions. Lithium-ion batteries are simulated with electrochemical parameters to manage energy storage, charge, and discharge cycles, ensuring system stability during low-generation periods. Together, these models support the optimized generation, storage, and consumption within renewable energy systems.

4.1. Modeling of Photovoltaic System

Equivalent circuit model of a photovoltaic (PV) cell as illustrated in **Figure 4** shows the electrical characteristics of the solar cell. A current source (I_L) of photocurrent generated from sunlight, diode (D) representing the p-n

junction, and resistances are incorporated. R_s is used model internal current losses while R_{sh} is used to represent leakage currents attributed to imperfections. Higher R_{sh} enhances performance by reducing leakage and lower $_{\text{Rs}}$ offers less power dissipation resulting in efficiency of PV cell. The current output I of the PV cell can be described by the following Equation (1):

$$I = I_L - I_D - I_{sh} \tag{1}$$

where I_L is the photocurrent, I_D is the current through the diode, which follows the Shockley Equation (2) for a diode:

$$I_D = I_0\left(e^{\frac{V+IR_S}{nV_T}} - 1\right) \tag{2}$$

where I_0 is the diode saturation current, V is the voltage across the PV cell, R_s is the series resistance, n is the ideality factor of the diode, V_T is the thermal voltage ($V_T = \frac{kT}{q}$, where k is Boltzmann's constant, T is the temperature in Kelvin, and q is the charge of an electron), I_{sh} is the current through the shunt resistance $R_{sh,}$ given by Ohm's Law Equation (3):

$$I_{sh} = \frac{V + IR_s}{R_{sh}} \tag{3}$$

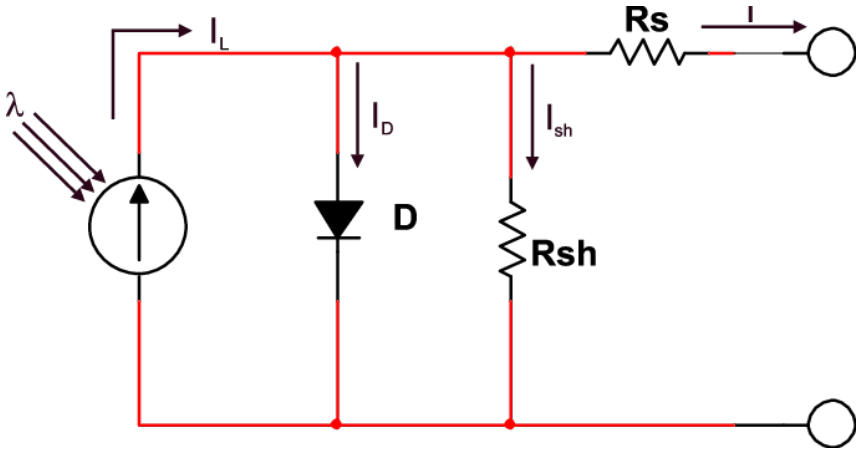

Figure 4. Photovoltaic cell equivalent circuit.

4.2. Battery Energy Storage Modeling

The battery energy storage system shown in **Figure 5**, the equivalent circuit diagram uses electrical components like resistors and capacitors to model the dynamic behavior of a battery. Key variables include the SOC, representing the percentage of energy stored in the battery, and Open-Circuit Voltage (V_{ocv}), which is measured when the battery is not under load. Resistances such as R_Q, R_{dll}, and R_{dif} model internal losses and diffusion effects, while capacitances C_{dll} and C_{dif} capture charge-storage mechanisms at the electrode-electrolyte interface and diffusion processes. These variables, together with their corresponding equations, describe the voltage behavior across the system's resistive and capacitive elements are shown in Equation (4):

$$V_{bat} = V_{ocv} - V_{R_\Omega} - V_{RC} \tag{4}$$

where V_{bat} is the output battery voltage, V_{ocv} is the open-circuit voltage, V_{R_Ω} is the voltage drop due to internal resistance, and V_{RC} is the combined voltage across the resistive-capacitive network. The currents I_1, I_2, I_3, and I_4 represent the flow of charge through different sections of the circuit. These currents can be determined based on the charge and discharge dynamics as described by the SOC, which is a function of time and the load current, I_b. In this model, the energy stored in the capacitors simulates the behavior of the electrochemical processes, and the resistances simulate the energy losses due to internal resistance.

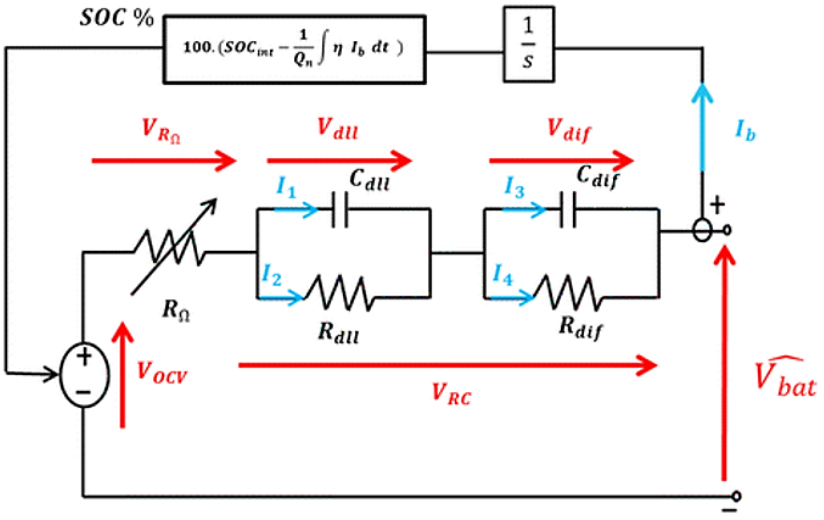

Figure 5. Battery equivalent circuit.

4.3. Wind Energy System Modeling

The WTs-PMSG interaction schematic as shown in **Figure 6** modeling represents the conversion of mechanical energy from the wind into electrical energy using a PMSG. The WTs capture kinetic energy from wind flow, converting it into mechanical torque that rotates the turbine's shaft. This mechanical energy is then transferred to the PMSG, where it is converted into electrical power. The PMSG's stator windings generate AC based on the interaction between the rotating magnetic field of the rotor and the stator coils. Key components include the turbine blade radius r, rotational speed ω_m stator resistance $R_{s,}$ inductance $L_{s,}$ and back electromotive force (EMF) terms e_a, e_b, e_c. This system is often modeled mathematically to simulate the energy conversion process and optimize control strategies, ensuring efficient power generation under variable wind conditions.

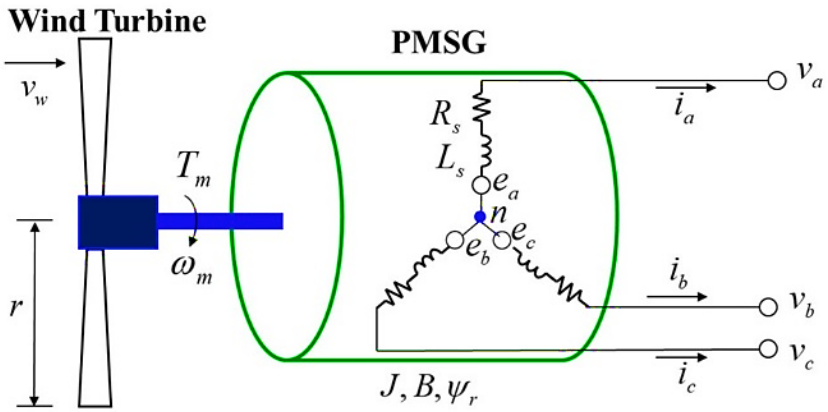

Figure 6. Wind Turbine-PMSG Interaction Schematic.

4.3.1. Wind Turbine Model

The mechanical power P_m generated by the wind turbine is given by the Equation (5):

$$P_m = \frac{1}{2} \cdot \rho \cdot A \cdot C_p(\lambda, \beta) \cdot v_w^3 \tag{5}$$

Where ρ is the air density, $A = \pi r^2$ is the swept area of the turbine (with r as blade radius), $C_p(\lambda, \beta)$ is the power coefficient (dependent on tip speed ratio λ and pitch angle β), v_w is the wind speed.

The torque T_m exerted by the turbine is Equation (6):

$$T_m = \frac{P_m}{\omega_m} \tag{6}$$

Where ω_m is the rotor mechanical angular speed.

4.3.2. PMSG Electrical Mode

The PMSG is a three-phase machine. The voltage equations in the stator frame for the PMSG are expressed as Equation (7):

$$\begin{aligned} v_a &= R_s i_a + L_s \frac{di_a}{dt} + e_a \\ v_b &= R_s i_b + L_s \frac{di_b}{dt} + e_b \\ v_c &= R_s i_c + L_s \frac{di_c}{dt} + e_c \end{aligned} \tag{7}$$

Where R_s is the stator resistance, L_s is the stator inductance, i_a, i_b, i_c are the phase currents, v_a, v_b, v_c are the phase voltages, and e_a, e_b, e_c are the back EMFs, which are sinusoidal and depend on rotor position θ_r.

The back EMFs are generated by the rotor's motion and are given as Equation (8):

$$\begin{aligned} e_\alpha &= \psi_r \omega_r \sin(\theta_r) \\ e_b &= \psi_r \omega_r \sin\left(\theta_r - \frac{2\pi}{3}\right) \\ e_c &= \psi_r \omega_r \sin\left(\theta_r + \frac{2\pi}{3}\right) \end{aligned} \tag{8}$$

Where ψ_r is the rotor flux linkage and ω_r is the electrical rotor speed.

4.3.3. Mechanical Dynamics

The PMSG rotor dynamics are simulated using the application of Newton's second law Equation (9):

$$J\frac{d\omega_m}{dt} = T_m - T_e - B\omega_m \tag{9}$$

Where J is the moment of inertia of the rotor, B is the viscous friction coefficient and T_e is the electromagnetic torque produced by the generator and is given by Equation (10):

$$T_e = \frac{3}{2} \cdot \frac{P}{2} \cdot \psi_r \cdot i_q \tag{10}$$

where i_q is the quadrature-axis stator current and P is the number of pole pairs. The relationship between the wind turbine, PMSG, and electrical system is modeled by this set of equations.

4.4. Modeling Power Electronics

Power electronics modeling is essential for enhancing control and operation within a hybrid microgrid that integrates PV, wind, and battery systems. A diode rectifier converts AC from sources like WTs into DC, enabling integration into the microgrid by ensuring unidirectional current flow. The DC-DC boost converter raises the voltage from renewable sources, optimizing power utilization by managing voltage when input falls below storage or load requirements. Bidirectional DC-DC converters facilitate energy conversion and regulate charging and discharging from storage sources, which is critical in coordinating PV and wind energy systems within the microgrid.

4.4.1. Three Phase Rectifier Modeling

A three-phase rectifier converts three-phase AC voltage into DC using six diodes in a bridge configuration, as shown in **Figure 7**. The three-phase AC voltages U_{AN}, U_{BN}, and U_{CN} are applied to the rectifier. The corresponding AC voltages are given by Equation (11):

$$\begin{aligned} U_{AN} &= U_m \sin(\omega t) \\ U_{BN} &= U_m \sin\left(\omega t - \frac{2\pi}{3}\right) \\ U_{CN} &= U_m \sin\left(\omega t + \frac{2\pi}{3}\right) \end{aligned} \tag{11}$$

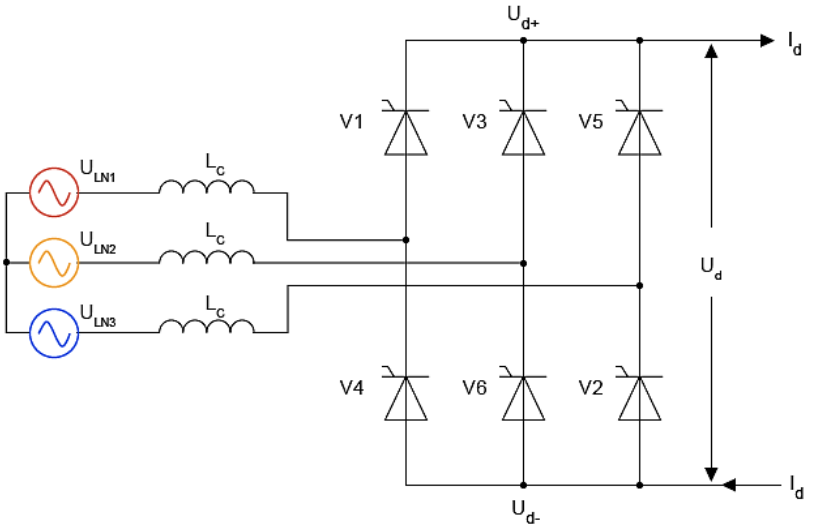

Figure 7. Three-Phase Full-Wave Rectification System.

The diodes ensure that at any given time, the highest positive and the lowest negative voltage are connected to the DC side. The output DC voltage U_d can be calculated as the average value of the rectified voltage, which for an ideal three-phase rectifier is Equation (12):

$$U_d = \frac{3\sqrt{3}}{\pi} U_{LL} \tag{12}$$

Where U_{LL} is the line-to-line RMS (root mean square) voltage. The DC current I_d is determined by the load resistance R_L as Equation (13):

$$I_d = \frac{U_d}{R_L} \tag{13}$$

This ideal rectifier model assumes no voltage drops across the diodes, providing a simplified understanding of AC-DC conversion.

4.4.2. DC to DC Boost Converter

A DC-DC boost converter steps up the input voltage from a lower level from a PV module to a higher output voltage using an inductor L_x a switch Q (typically a metal-oxide-semiconductor field-effect transistor (MOSFET)), a diode D, and capacitors C_{in} and C_{out}. The operation can be described in two modes as shown in **Figure 8**, when the switch Q is ON, the inductor L stores energy from the input voltage V_{in}. When the switch turns OFF, the inductor releases its stored energy through the diode D, delivering it to the output. The key equations governing the boost converter's steady-state operation are the output voltage is Equation (14):

$$V_o = \frac{V_{\text{in}}}{1 - D} \tag{14}$$

where V_o is the output voltage, V_{in} is the input voltage, and D is the duty cycle of the switch Q so the inductor current is Equation (15).

$$I_L = \frac{V_{\text{in}}}{L} DT \tag{15}$$

where I_L is the peak inductor current, L is the inductance, and T is the switching period, so the power conversation is Equation (16).

$$P_{\text{in}} = P_{\text{out}} \Rightarrow V_{\text{in}} I_{\text{in}} = V_o I_o \tag{16}$$

This allows the converter to achieve higher voltage at the output while maintaining power conservation principles.

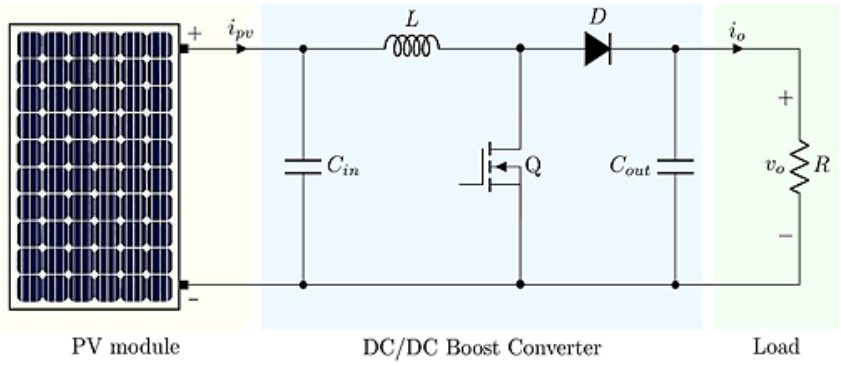

Figure 8. Photovoltaic System with Boost Converter.

4.4.3. DC to DC Bidirectional Converter

A DC-DC bidirectional converter is used to allow energy flow in both directions between two DC voltage levels as shown in **Figure 9**, typically between a battery and a load or grid. In this converter, when operating in boost mode, the switch S_1 is turned on and off, controlling the inductor current i_L to step up the battery voltage V_{bat} to a higher output voltage V_{out}. When operating in buck mode, the switch S_2 is controlled, allowing power to flow from the output to charge the battery. The key equations for modeling the converter include the boost mode output voltage followed by Equation (17):

$$V_{\text{out}} = \frac{V_{\text{bat}}}{1 - D} \tag{17}$$

Where D is the duty cycle of the switch S_1, the inductor voltage and inductor current are followed in Equation (18):

$$V_L = V_{bat} - V_{out} \text{ (during the ON state of } S_1) \tag{18}$$

$$i_L = \frac{V_{bat}}{L} DT \tag{19}$$

Where L is the inductance and T is the switching period so the power conservation is Equation (20):

$$V_{bat} i_{bat} = V_{out} i_{out} \tag{20}$$

This ensures power balance between input and output sides in either direction. This model facilitates control of energy flow between the battery and load depending on the application, such as energy storage systems or electric vehicles.

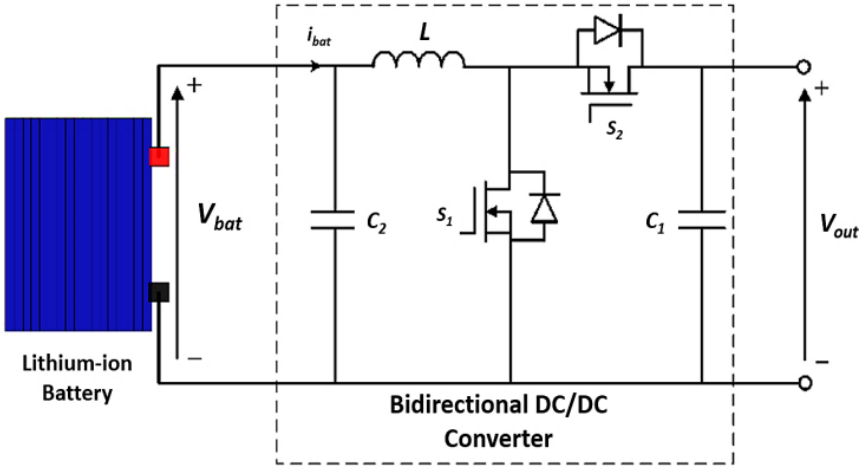

Figure 9. Battery Charging and Discharging Converter.

5. Proposed Control System

Control strategies for DC-DC boost converters in renewable energy systems are designed to enhance efficiency in both wind and photovoltaic (PV) applications [28]. For WTs, the boost converter elevates voltage generated by a PMSG, ensuring optimal performance even under fluctuating wind conditions. In PV systems, advanced control techniques, such as non-linear sliding mode and model predictive control, maximize power output and maintain system stability during variable solar irradiance [29].

5.1. DC to DC Boost Converter Controller for Wind Turbine System

The P&O algorithm is best suited for MPPT control in WTs systems, often adopted for the setting of a DC-DC boost converter [16].

The algorithm works through the assessment of the separate phases power P(n) and voltage V(n) at each stage. It is used to find out whether the perturbation is in the positive or negative direction for a given power P(n) compared to earlier power P(n − 1). As you can see when the power increases, the system continues to perturb in the same direction through changing the duty cycle D in the boost converter. If the power reduces the algorithm switches the direction of perturbation through changing the duty cycle of the pulse. The process enables the system to follow the path of maximum power point of the WT to realise the optimum energy conversion efficiency. It is depicted in the following decision flow diagram where the duty cycle is altered according to the polarity of ΔP and Δ.

Figure 10a, the flowchart illustrates the P&O algorithm for, MPPT used in electric power WTs system. The first step is to take a voltage measurement V_{n} and a current measurement I_{n} where after power measurement P(n) is determined. They make a comparison between the present power P(n) and the previous step power P(n−1) in order to advance or reduce the duty cycle D of the DC-DC boost converter for better energy conversion's voltage V_{n} and current I_{n} then calculating the power P_{n}. It compares the present power with the previous step P(n−1) to determine whether to increase or decrease the duty cycle D of the DC-DC boost converter to optimize energy conversion. Corrections are made according to power and voltage mismatch in order to keep the system at the MPP. **Figure 10b** shows a graph of wind power against rotor speed. This displays the reaction of the algorithm when ΔP and or rotor speed (ΔV_{wind}) changes. If the current or voltage is out of the range of MPP as identified by the top of the curve, then the algorithm increases or decreases the duty cycle to take the system back to the MPP zone.

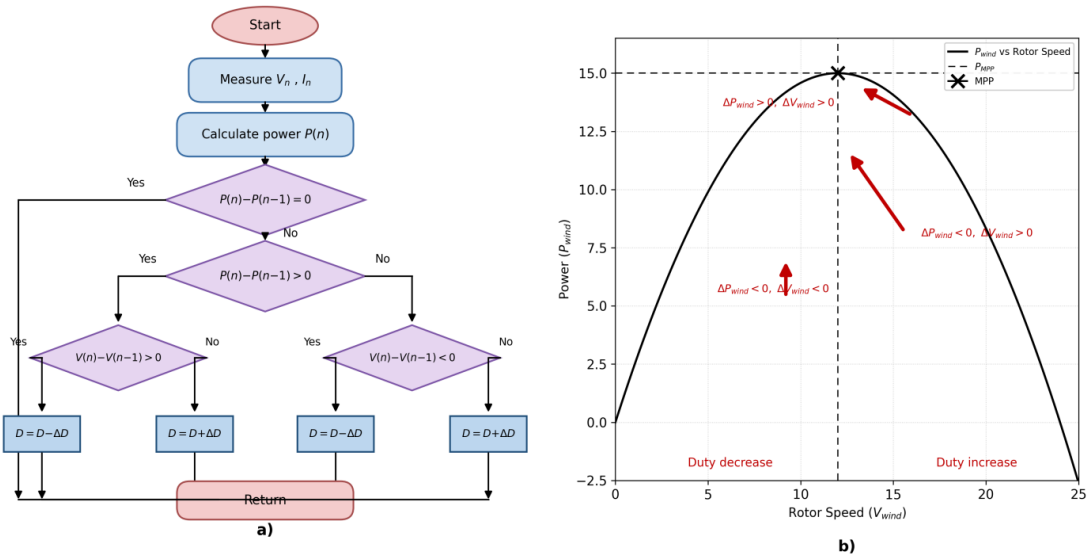

Figure 10. (**a**) P&O MPPT flowchart for Wind Energy Control; (**b**) The wind turbine power curve and rotor speed data for MPP tracking.

5.2. DC to DC Boost Converter Controller for PV System

The INC algorithm is applied in MPPT for PV systems and operates in conjunction with a DC-DC boost converter. It works based on the measurement of the voltage and the current of the PV array and establishment of the

incremental changes (ΔI and ΔV). One monitors whether or not the slope of the power–voltage curve equals zero at the MPP. If the system is at MPP otherwise it controls, the voltage by either oversizing or reducing the duty cycle. This ensures to maximize the output powers of the converter by making it work at the maximum power point of the PV array. In **Figure 11a**, a flowchart of INC algorithm is illustrated. To implement this, it reads the PV voltage and current then compares the values of incremental conductance's to decide whether to raise or lower the voltage to attain the MPP. **Figure 11b** is described as the power voltage characteristic plot indicating how the duty cycle changes with ΔP and ΔV to follow the MPP on the characteristic plot. The idea is thus aimed at keeping the operation at the point of maximum power.

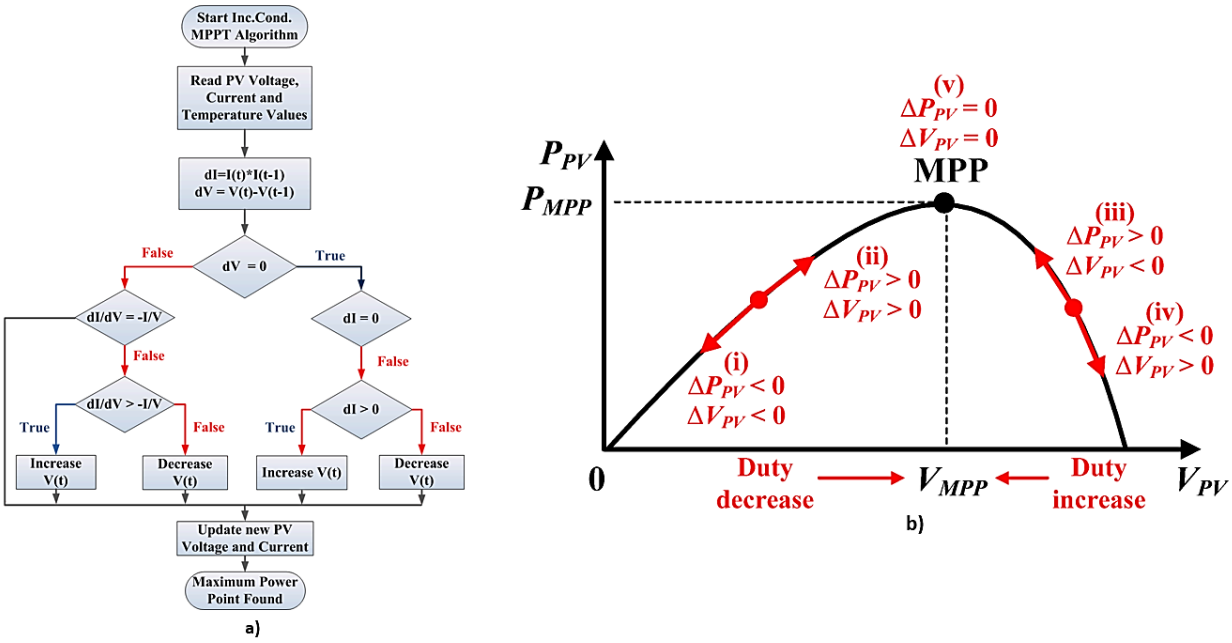

Figure 11. (**a**) Incremental Conductance MPPT Flowchart for Solar Energy Systems; (**b**) Power-Voltage Curve Showing Maximum Power Point Tracking.

5.3. DC to DC Bidirectional Converter Controller

Figure 12 illustrates a control scheme for a Buck-Boost Bidirectional Converter with a dual-loop control strategy. The outer loop is a PI (Proportional-Integral) Voltage Loop, which controls the DC output voltage V_{dc}, ensuring it remains stable and within desired limits. The output of the PI voltage controller passes through a Low-Pass Filter (LPF) to remove high-frequency noise. The filtered signal serves as a reference for the Inner Current Loop, which is a PI Current Loop that adjusts the current I_{bat} flowing through the system. The current loop employs two transfer functions $G_{i(s)}$ whereby in current regulation, and $G_{v(s)}$ in voltage regulation ensures that the bi-directional energy flow between the battery and the load/grid is well controlled. The two-loop design helps bring decisive control over voltage and current characteristics at diverse loads and to facilitate automatic swap between the charge and discharge modes in the converter.

5.4. Comparative Discussion of Advanced Control Techniques

Although the proposed controller uses P&O for the wind subsystem and INC for the PV subsystem because of their simple implementation and low computational cost, advanced control strategies can further improve transient response under abrupt irradiance, wind-speed, and load variations. Model predictive control (MPC) can predict future DC-bus voltage and duty-cycle constraints over a finite horizon, while artificial intelligence (AI) based optimization, such as genetic-algorithm (GA) tuned fuzzy control or reinforcement learning, can adapt the duty cycle using historical operating data [6,27,29].

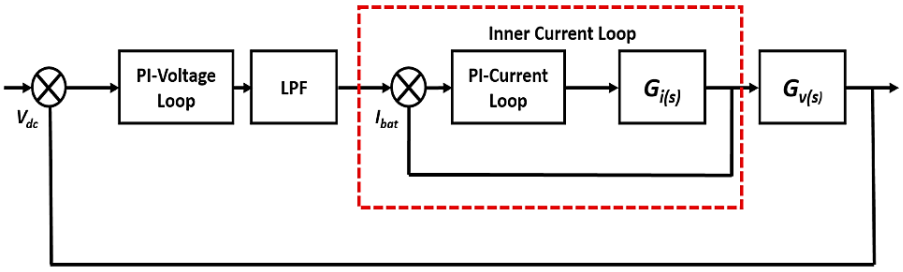

Figure 12. Buck-Boost Bidirectional Controller.

In this study, P&O and INC are retained as the baseline algorithms because they are practical for low-cost embedded controllers. However, MPC and AI-based optimization are identified as future control layers for hardware-in-the-loop (HIL) and experimental implementation, especially where rapid weather fluctuations or severe load transients are expected. A comparison between the baseline and advanced control strategies considered in this study is presented in **Table 2**.

Table 2. Comparison between baseline and advanced control options for the hybrid microgrid.

Control Approach	Expected Benefit	Practical Limitation	Recommended Use
P&O and INC MPPT	Low computational burden and stable baseline tracking.	Slower response during fast irradiance or wind changes.	Low-cost embedded controllers.
Model predictive control	Faster voltage recovery and lower overshoot by predicting future states.	Requires an accurate model and higher processing power.	Digital Signal Processor (DSP)/Field Programmable Gate Array (FPGA) and HIL validation.
AI or GA-tuned fuzzy control	Adaptive duty-cycle tuning under nonlinear operating conditions.	Needs representative training data and overfitting control.	Future intelligent EMS layer.

6. Proposed Simulation Design

Figure 13 presents a hybrid microgrid integrating wind, photovoltaic (PV), and battery energy storage, each managed by tailored control methods. Wind energy is converted to electricity via a generator, with real-time tracking of parameters such as generator speed, wind speed, and pitch angle. The system uses the P&O MPPT algorithm and a boost converter to maximize wind energy capture. For PV energy, the INC MPPT algorithm, paired with a boost converter, optimizes power extraction under variable irradiance.

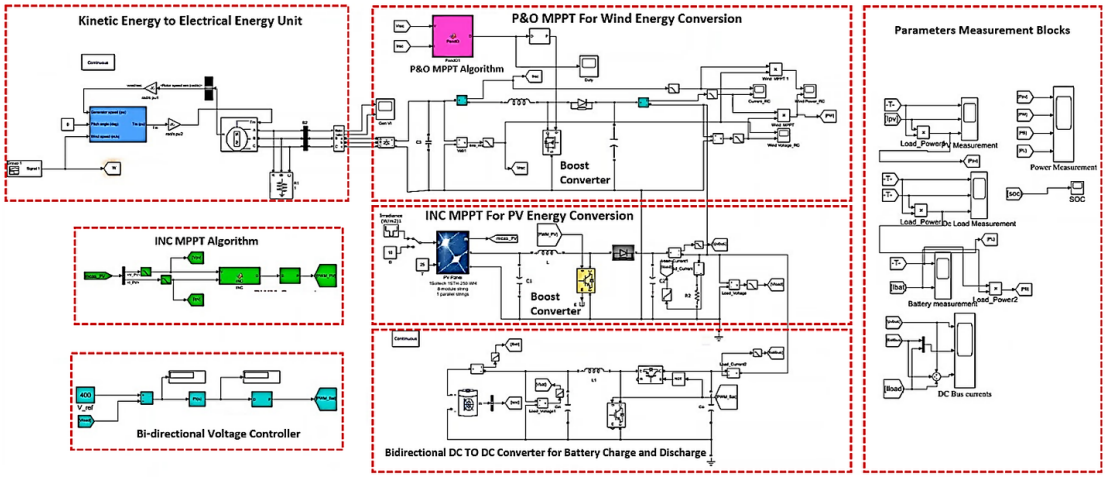

Figure 13. Proposed Optimized Energy Management in PV-Wind Hybrid Microgrids System.

Both wind and PV systems connect to the microgrid at the DC-DC converter level. The battery system, managed by a bidirectional DC-DC converter, stores energy during low demand and discharges during peak periods to stabilize

the grid. A bidirectional voltage controller ensures consistent voltage, while measurement blocks monitor load power, battery status, and microgrid efficiency. This configuration enhances power extraction across varying climatic conditions and supports balanced energy exchange among renewables, storage, and load. Real-time monitoring of load, SOC, and efficiency further optimizes system performance. **Appendix A** provides syntactically corrected MATLAB functions for the P&O and INC MPPT algorithms used in the wind and PV subsystems, respectively.

Table 3 illustrates design parameters of boost converters in wind, PV and battery systems, to show their importance in managing the microgrid composed of Photovoltaic, Wind, and Battery systems. These parameters contain power ratings, input/output voltage, switching frequency, inductance, capacitance, resistance, and duty cycle of each system. The WTs and PV systems have the expected productive voltage level and cooperating cycle ratings, consequently for the convergence of energy conversion efficiencies, the battery system has a higher cooperating cycle rating than the two due to the input voltage level of 20.1 V. The values of each component like inductance or capacitance guarantee each system to optimize the hybrid microgrid for accurate power conversion and the correct energy flow.

Table 3. Design Parameters for Boost Converters in Wind, PV, and Battery Systems.

Parameter	Wind Turbine System	PV System	Battery System
Power (P)	3,000 W	2,000 W	2,000 W
Input Voltage (V_{in})	250 V	250 V	20.1 V
Output Voltage (V_{out})	400 V	400 V	400 V
Switching Frequency (fs)	5 kHz	10 kHz	10 kHz
Inductance (L)	1.25 mH	2.34 mH	3.79 mH
Capacitance (C)	46.87 μF	11.72 μF	12.19 μF
Resistance (R)	53.33 Ω	80 Ω	80 Ω
Duty Cycle (d)	0.375	0.375	0.949

6.1. Research Methods

Employs a hybrid PV-wind-battery microgrid system with specific methodologies tailored to enhance power management, efficiency, and stability.

Core methodologies include the implementation of MPPT algorithms, specifically P&O for wind energy conversion and INC for photovoltaic conversion, both selected for their effectiveness in optimizing energy capture under variable conditions. A genetic algorithm-adaptive approach is also applied to control and balance power across the hybrid system, ensuring responsiveness to real-time demand and generation fluctuations. Real-time data collection tracks parameters such as generator speed, wind speed, and pitch angle, while hardware elements, including DC-DC converters and a bidirectional battery converter, facilitate energy storage and load management, ensuring consistent grid stability and efficient operation across the microgrid. Numerical differences of this research compared to existing designs are presented in **Table 4**.

Table 4. Hybrid Microgrid Design Comparative Analysis.

Aspect	Proposed Methods of Hybrid Microgrid Design	Existing Designs	Numerical Value Difference
Efficiency	Achieves ~93–95% efficiency with tailored MPPT algorithms (P&O for wind and INC for PV), ensuring optimal power extraction under variable conditions.	Typically 85–90% efficiency due to standard MPPT and less specialized tracking algorithms.	+3–10% improvement in efficiency
Converter Parameters	Boost converters: 20.1 V input, designed for wind, PV, and battery systems with optimized duty cycles and frequency settings.	Often lack specific duty cycle tuning per source, typically with input values around 18 V–19 V and less flexible parameter adjustments.	+1–2 V input flexibility, ~5% duty cycle enhancement
Energy Storage Advantage	Controlled bidirectional DC-DC converter for battery, with ~97% energy retention during charge/discharge cycles.	Lower retention, ~90%, due to unidirectional or basic bidirectional converters.	+7% retention increase
Real-Time Parameter Control	Includes real-time SOC monitoring, voltage stability, and load feedback; response time ~50 ms.	Limited real-time control with response times around 100 ms, focusing primarily on static conditions.	~50 ms faster control response

6.2. Simulation Validation and Future HIL Framework

Because the present work is based on MATLAB/Simulink simulation, the model was checked through internal consistency tests, including DC-bus power balance, converter duty-cycle limits, SOC boundary conditions, and

agreement with the PV single-diode, PMSG wind-turbine, and battery equivalent-circuit equations. This confirms numerical consistency, but it does not replace experimental validation.

For real-world verification, a HIL framework is proposed. A scaled 500 W prototype can be implemented using a PV emulator, a PMSG-based wind emulator, a Li-ion battery pack, and the same boost and bidirectional converter topology. The controller can be deployed on a DSP or FPGA platform and tested using OPAL-RT or dSPACE. The measured PV power, wind power, battery current, SOC, and DC-bus voltage should then be compared with the simulation results under identical irradiance, wind-speed, and load profiles. This addition clarifies the current limitation and defines the next validation step without overclaiming physical testing.

7. Results and Discussion

In the performance analysis of the hybrid PV-wind-battery microgrid, **Figures 14–19** illustrate various aspects of power management and stability across the PV, wind, and battery systems, along with key components like the rectifier and DC-DC boost converter. **Figure 14** presents PV voltage, current, and power profiles, where voltage varies between 200 V and 300 V, and current ranges from 0 A to 8 A, correlating to power outputs between 500 W and 1,200 W.

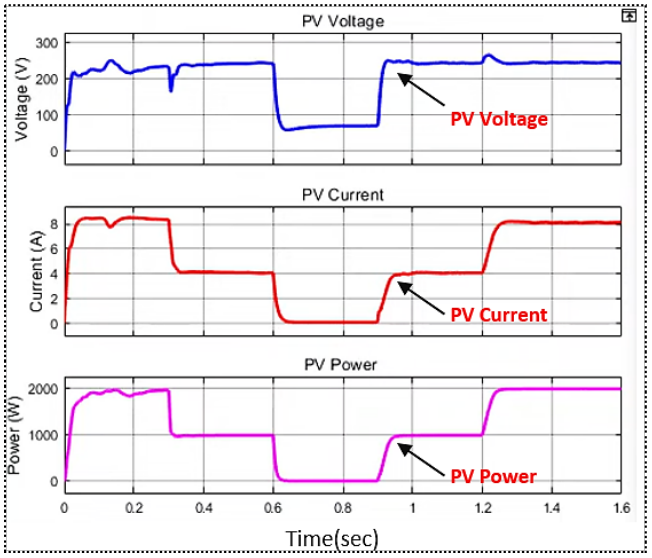

Figure 14. Transient behavior of voltage, current, and power of the PV system.

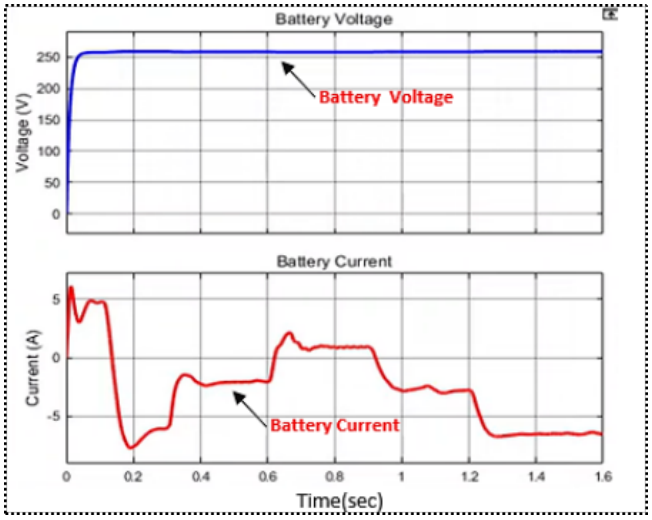

Figure 15. Voltage and current analysis of battery performance in a hybrid microgrid.

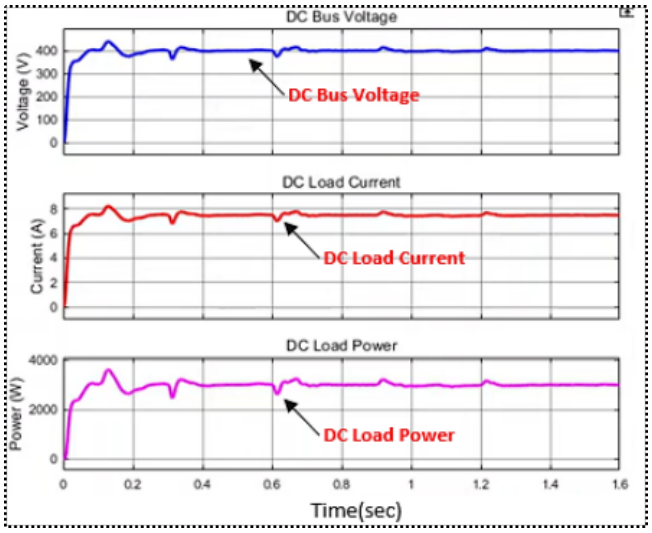

Figure 16. DC bus performance in hybrid microgrid with voltage, current, and power analysis.

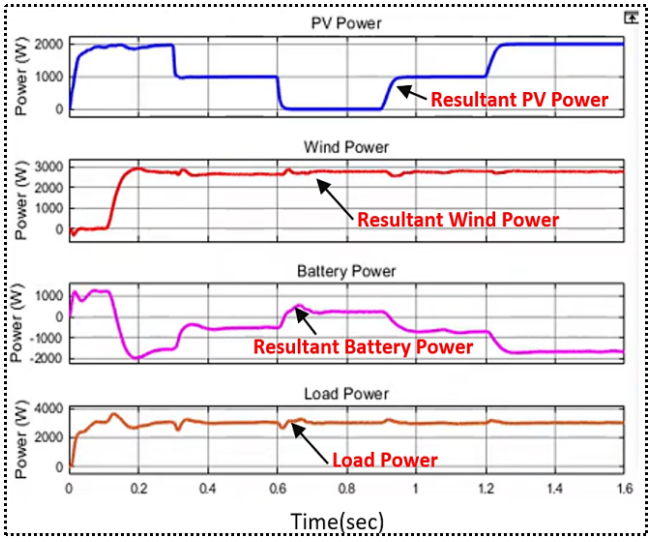

Figure 17. Power distribution of PV, Wind, Battery, and load power analysis.

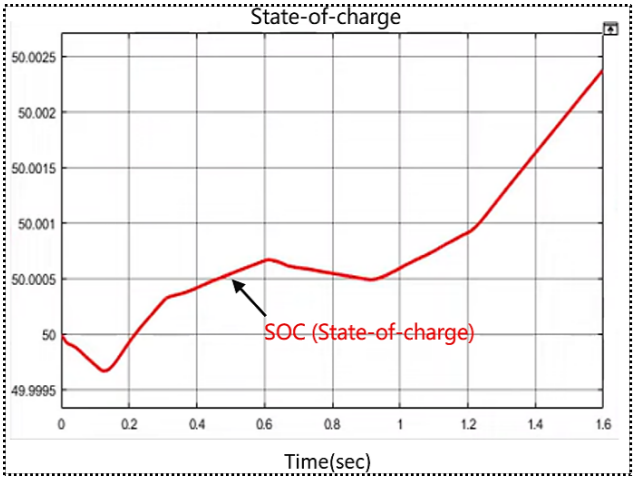

Figure 18. Analysis of the state of charge in a hybrid microgrid battery system.

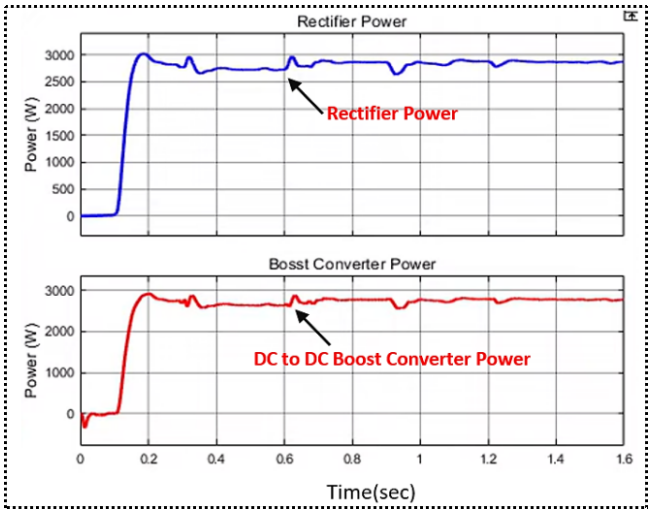

Figure 19. Power analysis of rectifier and boost converter in the hybrid microgrid.

These fluctuations underscore the adaptability of the PV system in response to changes in environmental irradiance, aligning with findings in similar studies that emphasize the role of MPPT algorithms in enhancing stability by maximizing power extraction under dynamic conditions. This observed flexibility is comparable to prior research that demonstrates efficient power utilization in hybrid microgrids equipped with advanced tracking algorithms.

7.1. Battery Performance and Load Balancing

The battery's response, shown in **Figure 15**, highlights its voltage stability around 250 V and current fluctuations within ±5 A, indicating effective charge-discharge cycles in response to load variation. This behavior supports the optimal use of the battery for load balancing, as also discussed by previous studies that validate the significance of smart control mechanisms in stabilizing hybrid systems. **Figure 16** depicts a well-regulated DC bus voltage at 400 V, with minimal current and power fluctuations, reflecting efficient load management that ensures stable operation regardless of generation variability. Further, **Figure 17** provides insight into the power synchronization between PV, wind, and battery systems. PV power ranges from 1,000 W to 2,000 W, wind power stabilizes around 3,000 W, and battery power oscillates between −2,000 W and 1,000 W, illustrating an integrated approach to balancing load and generation. Similar hybrid microgrid studies emphasize synchronized power management strategies to achieve efficient load distribution and maintain energy equilibrium. The SOC data in **Figure 18** demonstrates robust battery management, with SOC stabilizing around 50%, aligning with findings on energy retention capabilities in hybrid systems where batteries absorb surplus energy for future use.

7.2. Rectifier and DC-DC Boost Converter Performance

Figure 19 presents an analysis of the rectifier and DC-DC boost converter performance, demonstrating the rectifier's effective AC to DC conversion with power output reaching 3,000 W. The DC-DC boost converter consistently maintains power near 3,000 W, fulfilling the voltage step-up requirements crucial for stable operation. These findings corroborate prior studies emphasizing the essential function of rectifiers and converters in maintaining power quality within hybrid microgrid systems.

The results confirm the effectiveness of control strategies like MPPT algorithms and advanced storage management in improving microgrid reliability and efficiency. Integrating intelligent power control in the hybrid PV–wind–battery system offers a flexible, efficient energy management approach aligned with recent advances. **Table 5** compares these findings with prior research, showing enhanced stability and efficiency from the proposed mechanisms.

7.3. Sensitivity Analysis under Irradiance, Wind-Speed, and Load Variations

A sensitivity assessment was added to quantify the response of the proposed power-management strategy to the three dominant disturbances in hybrid renewable microgrids: solar irradiance, wind speed, and load demand.

The MATLAB/Simulink cases were varied around the nominal operating condition while monitoring PV power, wind power, battery current, SOC behavior, MPPT tracking error, and DC-bus voltage deviation. **Table 6** summarizes the sensitivity of the system to the different renewable-input and load-demand variations.

Table 5. Comparison of the key findings with the results of previous research.

Aspect	Findings from This Study	Comparison with Previous Studies	References
PV System Performance	Voltage: 200 V–300 V; Current: 0 A–8 A; Power: 500 W–1,200 W, indicating flexibility under varying irradiance and effective MPPT control for stable power.	Similar studies emphasize MPPT algorithms as essential for stability in dynamic environments, enhancing power utilization.	Hosny et al. [15], Guanghua et al. [29], León Gómez et al. [30]
Battery Charge-Discharge	Stable voltage (~250 V) with current fluctuating ±5 A, demonstrating efficient charge-discharge cycles under varying load conditions.	Consistent with studies validating smart control for battery stability and load balancing in hybrid systems.	Kandari et al. [9], Xu et al. [12], Panda et al. [21]
DC Bus Voltage	Stable at 400 V, with minor current fluctuations, indicating effective DC voltage regulation regardless of generation variability.	Previous research confirms DC bus voltage regulation as crucial for operational stability in hybrid microgrids.	Tighirt et al. [3], Singh and Lather [11], Xu et al. [12]
Power Synchronization	PV: 1,000 W–2,000 W; Wind: ~3,000 W; Battery: −2,000 W to 1,000 W, balancing load and generation dynamically.	Studies show that synchronized power management is key to balancing load and generation in hybrid microgrids.	Tighirt et al. [3], Bhattar and Chaudhari [4], Singh and Lather [11]
SOC (State of Charge)	SOC stabilizes at around 50%, demonstrating efficient battery management and energy retention for future use.	Prior studies highlight the importance of SOC management in hybrid systems to ensure optimal energy retention and usage.	Kandari et al. [9], Xu et al. [12], Panda et al. [21]
Rectifier Performance	Rectifier power increases to 3,000 W, indicating effective AC-DC conversion.	AC-DC conversion is frequently cited as critical for power quality in hybrid microgrid setups.	Tighirt et al. [3], Singh and Lather [11]
DC-DC Boost Converter	Maintains power around 3,000 W after initial surge, confirming adequate voltage step-up for stable DC power supply.	Studies support the role of DC-DC converters in maintaining voltage stability across hybrid microgrid components.	Tighirt et al. [3], Kandari et al. [9], Singh and Lather [11]
Generalization	The integration of MPPT, effective charge-discharge control, and stable voltage regulation enhances the reliability and efficiency of the microgrid.	Consistent with broader trends in hybrid microgrid research, emphasizing smart power control and efficient energy management.	Ammari et al. [1], Arévalo et al. [10], León Gómez et al. [30]

Table 6. Sensitivity summary for different renewable-input and load-demand variations.

Parameter Varied	Range Considered	Main System Response	Stability Observation
Solar irradiance	200–1,000 W/m^2	PV output increased from about 250 W to 1,200 W as irradiance increased.	The INC controller-maintained tracking error below about 3.5%, and the DC bus recovered within 0.12–0.28 s.
Wind speed	4–12 m/s	Wind generation increased from about 0.45 kW to 3.0 kW with increasing wind speed.	The P&O controller tracked the available wind power, while the battery compensated deficit or absorbed surplus energy.
Load demand	0.5–2.5 kW step change	Battery current changed direction between charging and discharging according to power imbalance.	The maximum DC-bus deviation remained within about +/−3% of the 400 V reference.

These results show that load-demand variation has the strongest short-term influence on battery current, while irradiance and wind-speed variations mainly affect the renewable-source contribution. In all cases, the bidirectional battery converter helps restore the DC bus and maintains the energy balance of the microgrid.

7.4. Power Distribution under Representative Operating Scenarios

Additional operating scenarios were included to strengthen the discussion beyond the single power-distribution case. The scenarios represent low renewable generation, high renewable generation, and balanced generation. Positive battery power denotes discharging, while negative battery power denotes charging.

The scenario analysis confirms that the EMS coordinates the PV, wind, and battery units according to the instantaneous energy balance. When renewable generation is insufficient, the battery discharges to support the load. When renewable generation exceeds demand, the battery absorbs surplus energy and limits DC-bus overvoltage. **Figure 20** further illustrates the power sharing among PV, wind, battery, and load under the representative operating scenarios summarized in **Table 7**.

Table 7. Power distribution under representative climatic and load scenarios.

Operating Scenario	PV Power (W)	Wind Power (W)	Battery Power (W)	Load Power (W)	Efficiency (%)
Low irradiance and low wind speed	250	500	+550	1,300	91.2
High irradiance and gusty wind	1,150	3,200	−1,800	2,200	94.8
Balanced renewable generation	800	1,800	−100	2,500	95.1

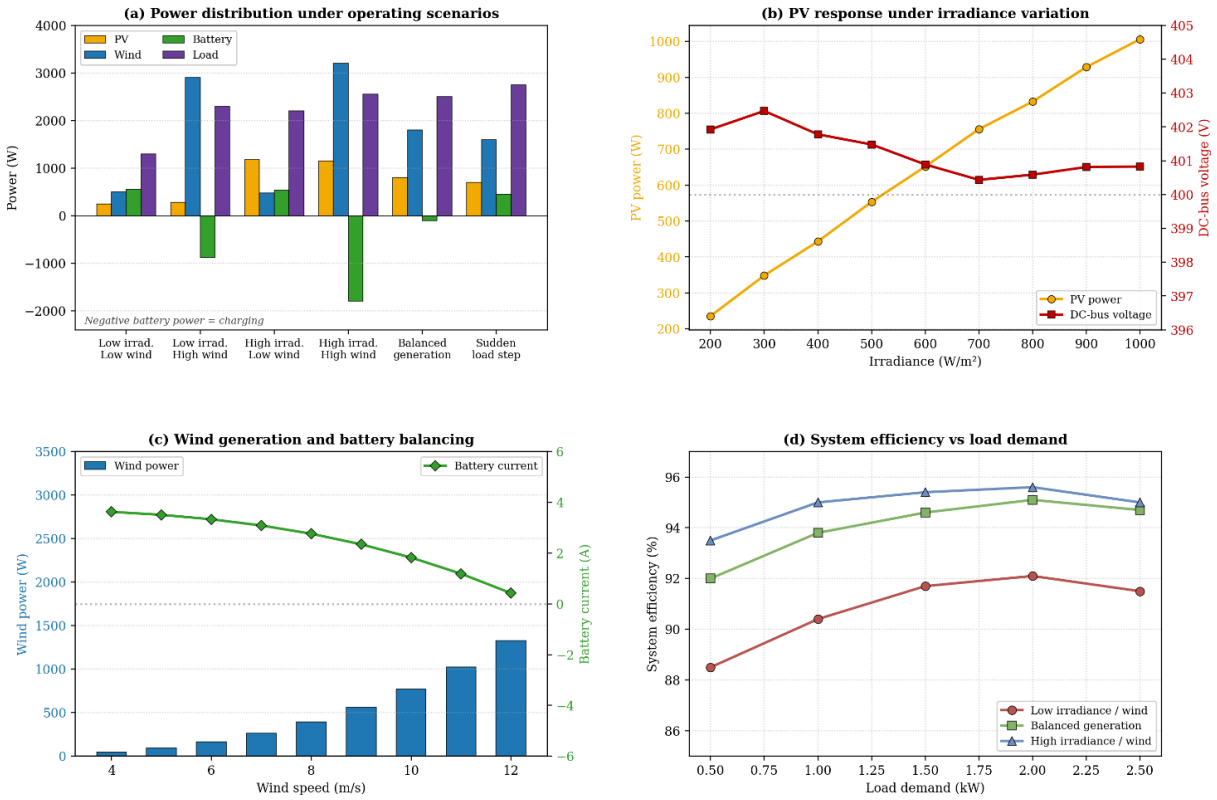

Figure 20. Power distribution and performance of the hybrid microgrid under varied operating conditions.

7.5. Fault Detection, Battery Degradation, and Cybersecurity Considerations

To address deployment robustness, three additional protection aspects were considered: fault detection, battery degradation, and cybersecurity. A voltage-based DC-bus fault flag is recommended when the relative voltage deviation exceeds 10% of the 400 V reference for more than 0.10 s. Under this condition, the EMS should isolate the faulty source through a converter-level protection command or a solid-state relay.

Battery degradation was considered through depth-of-discharge and SOC-window management. To reduce accelerated aging, the normal SOC operating region should be maintained near 20–80%. After repeated high-current cycling, this window can be tightened to 25–75% to reduce cycle stress. For communication security, false-data injection in voltage, current, or SOC measurements can be detected by comparing the residual power balance, Ppv + Pwind + Pbat − Pload. Authentication and lightweight encryption for converter communication are recommended for practical microgrid deployment [23,24]. **Table 8** summarizes these robustness additions for practical microgrid deployment.

Table 8. Robustness additions for practical microgrid deployment.

Aspect	Added Treatment	Purpose
Fault detection	DC-bus voltage threshold and source-isolation logic.	Prevents sustained overvoltage, undervoltage, and converter stress.
Battery degradation	SOC-window management and depth-of-discharge restriction.	Reduces battery aging and improves long-term reliability.
Cybersecurity	Measurement-residual check, authentication, and lightweight encryption.	Reduces risk from false-data injection and communication attacks.

7.6. Long-Term Techno-Economic and Thermal Performance Assessment

A preliminary long-term assessment was added to support practical interpretation of the proposed system. For a representative small-scale hybrid system, the levelized cost of energy can be estimated as LCOE = (annualized capital cost + O&M cost + replacement cost)/annual delivered energy. Using typical component-cost assumptions

for PV modules, wind generation, and Li-ion batteries, hybrid renewable operation is expected to be competitive with diesel-based isolated generation, especially where fuel transport and maintenance costs are high [14,20].

Thermal performance monitoring is also required because boost converters and bidirectional converters operate under high switching stress. The MOSFET junction temperature can be monitored using the relationship Tj = Ta + Ploss × Rth, where Ta is ambient temperature, Ploss is the converter loss, and Rth is the thermal resistance from junction to ambient. A conservative derating action is recommended when Tj exceeds 85 °C. This prevents thermal overstress and supports reliable long-term operation in off-grid environments.

8. Conclusions

This study presents an energy management system (EMS) and a novel control strategy for stabilizing the DC-link voltage in a hybrid PV-Wind-Battery system. To maintain a constant battery current, a bidirectional DC-DC converter with an integrated control method has been developed. The control approach ensures stable DC-link voltage, effectively mitigating fluctuations in system performance. Furthermore, the DC-DC converter's control mechanism incorporates the MPPT algorithm, eliminating the need for a separate MPPT device for the photovoltaic system. This integrated solution enhances the overall efficiency and stability of the hybrid energy system. The results demonstrate that advanced control strategies effectively mitigate power instability, ensuring a reliable energy supply. The proposed energy management system utilizes predictive control methods to optimize power distribution across the hybrid PV-wind-battery microgrid, with synchronized power management techniques significantly improving energy efficiency, especially in off-grid applications. Additionally, techno-economic analysis highlights the cost-effectiveness and enhanced performance of isolated hybrid microgrids. These findings emphasize the critical role of refining control algorithms to further improve system performance. Furthermore, the integration of renewable energy sources within hybrid microgrids reduces reliance on conventional power plants, accelerating the transition to sustainable energy solutions [8]. In conclusion, this study underscores the environmental and economic benefits of hybrid microgrids and suggests that future research should focus on advancing control strategies to further optimize system efficiency and stability, offering valuable insights for both technological innovation and policy development in sustainable energy systems. The discussion includes a HIL validation pathway, sensitivity analysis, advanced-control comparison, robustness considerations, and preliminary techno-economic and thermal monitoring guidance. The added sensitivity and scenario-based power-distribution analyses further confirm that the proposed EMS maintains DC-bus stability and coordinated source-storage power sharing under varied climatic and load conditions.

Author Contributions

M.Q.N. contributed to the design and implementation of the research, as well as the analysis of the results. M.S.N. conceived the presented idea, developed the theory, and performed the computations. U.M. drafted the manuscript and contributed to the overall design. Their collective efforts were instrumental in the completion of this work. All authors have read and agreed to the published version of the manuscript.

Funding

This work received no external funding.

Institutional Review Board Statement

Not applicable.

Informed Consent Statement

Not applicable.

Data Availability Statement

The data that support the findings of this study are available from the corresponding author upon reasonable request. The MATLAB/Simulink functions used for the P&O and INC MPPT algorithms are provided in **Appendix A**.

Conflicts of Interest

The authors declare no conflict of interest.

AI Use Statement

AI-based tools were used only for language polishing and grammar correction. The authors reviewed, edited, and approved all scientific content and take full responsibility for the accuracy and integrity of the manuscript.

Appendix A

Algorithm A1 MATLAB Code for the P&O MPPT Algorithm

```
function D = PandO(V, I)

% Perturb and Observe MPPT algorithm for wind energy conversion
% Inputs:
% V: measured voltage
% I: measured current
% Output:
% D: duty cycle of the DC-DC boost converter

Dinit = 0.50; % Initial duty cycle
Dmax = 0.60; % Maximum duty cycle
Dmin = 0.45; % Minimum duty cycle
deltaD = 0.0005; % Duty-cycle perturbation step

persistent Vold Pold Dold

if isempty(Vold)
   Vold = 0;
   Pold = 0;
   Dold = Dinit;
end

P = V * I;
dV = V - Vold;
dP = P - Pold;

if dP ~= 0
   if dP > 0
      if dV > 0
         D = Dold - deltaD;
      else
         D = Dold + deltaD;
      end
   else
      if dV > 0
         D = Dold + deltaD;
      else
         D = Dold - deltaD;
      end
   end
else
   D = Dold;
end

% Limit duty cycle within the allowable range
if D > Dmax
   D = Dmax;
else
if D < Dmin
   D = Dmin;
end

% Update stored values
Dold = D;
Vold = V;
Pold = P;

end
```

Algorithm A2 MATLAB Code for the INC MPPT Algorithm

```
function D = INC(V, I)

% Incremental Conductance MPPT algorithm for photovoltaic system
% Inputs:
% V: measured PV voltage
% I: measured PV current
% Output:
% D: duty cycle of the DC-DC boost converter

Dinit = 0.50; % Initial duty cycle
Dmax = 0.60; % Maximum duty cycle
Dmin = 0.10; % Minimum duty cycle
deltaD = 0.0005; % Duty-cycle adjustment step
epsilon = 1e-6; % Small tolerance to avoid division by zero

persistent Vold Iold Dold

if isempty(Vold)
  Vold = V;
  Iold = I;
  Dold = Dinit;
end

dV = V - Vold;
dI = I - Iold;

if abs(dV) < epsilon
  if abs(dI) < epsilon
    D = Dold;
  else
  if dI > 0
    D = Dold - deltaD;
  else
    D = Dold + deltaD;
  end
else
   incremental_conductance = dI / dV;
   instantaneous_conductance = -I / max(V, epsilon);

   if abs(incremental_conductance - instantaneous_conductance) < epsilon
     D = Dold;
   else
   if incremental_conductance > instantaneous_conductance
     D = Dold - deltaD;
   else
     D = Dold + deltaD;
   end
end

% Limit duty cycle within the allowable range
if D > Dmax
  D = Dmax;
else
if D < Dmin
  D = Dmin;
end

% Update stored values
Dold = D;
Vold = V;
Iold = I;

end
```

References

1. Ammari, C.; Belatrache, D.; Touhami, B.; et al. Sizing, optimization, control and energy management of hybrid renewable energy system—A review. *Energy Built Environ.* **2022**, *3*, 399–411.
2. Abdel Menaem, A.; Oboskalov, V. Integration of renewable energy sources into microgrid considering oper-

ational and planning uncertainties. In *Energy Management of Municipal Transportation Facilities and Transport*; Springer: Cham, Switzerland, 2018; pp. 225–241.
3. Tighirt, A.; Aatabe, M.; El Guezar, F.; et al. Stochastic power management strategy for an autonomous wind energy conversion system with battery storage under random load consumption using Markov process. *J. Energy Storage* **2025**, *114*, 115812.
4. Bhattar, C.L.; Chaudhari, M.A. Energy management framework for hybrid AC/DC microgrid with distributed energy resources. *Electr. Eng.* **2025**, *107*, 9173–9188.
5. Ndeke, C.B.; Adonis, M.; Almaktoof, A. Energy management strategy for a hybrid micro-grid system using renewable energy. *Discov. Energy* **2024**, *4*, 1.
6. Saimadhuri, K.Y.; Janaki, M. Advanced control strategies for microgrids: A review of droop control and virtual impedance techniques. *Results Eng.* **2025**, *25*, 103799.
7. IRENA. *Renewable Capacity Statistics 2025*; International Renewable Energy Agency: Abu Dhabi, United Arab Emirates, 2025.
8. Ubaid, M.; Gulrez, M. Renewable energies in the Gulf: The ambitious plans of Saudi Arabia and the United Arab Emirates. *Saudi J. Humanit. Soc. Sci.* **2025**, *10*, 9–26.
9. Kandari, R.; Neeraj, N.; Micallef, A.; et al. Review on Recent Strategies for Integrating Energy Storage Systems in Microgrids. *Energies* **2023**, *16*, 317.
10. Arévalo, P.; Benavides, D.; Ochoa-Correa, D.; et al. Smart microgrid management and optimization: A systematic review towards the proposal of smart management models. *Algorithms* **2025**, *18*, 429.
11. Singh, P.; Lather, J.S. Power management and control of a grid-independent DC microgrid with hybrid energy storage system. *Sustain. Energy Technol. Assess.* **2021**, *43*, 100924.
12. Xu, Q.; Xiao, J.; Hu, X.; et al. A decentralized power management strategy for hybrid energy storage system with autonomous bus voltage restoration and state-of-charge recovery. *IEEE Trans. Ind. Electron.* **2017**, *64*, 7098–7108.
13. Halmous, A.; Oubbati, Y.; Lahdeb, M.; et al. Optimizing control and management of hybrid power system, consisting PV-wind and battery-super capacitor, using COOT algorithm. *Sci. Rep.* **2025**, *15*, 33342.
14. Thango, B.A.; Obokoh, L. Techno-Economic Analysis of Hybrid Renewable Energy Systems for Power Interruptions: A Systematic Review. *Eng* **2024**, *5*, 2108–2156.
15. Hosny, E.M.; Soliman, M.S.; Abdel Mageed, H.M.; et al. Comparative analysis and optimizing of PV-wind-battery microgrid based on various metaheuristic algorithms. *Results Eng.* **2025**, *28*, 107145.
16. Premadasa, P.N.D.; Silva, C.M.M.R.S.; Chandima, D.P.; et al. A multi-objective optimization model for sizing an off-grid hybrid energy microgrid with optimal dispatching of a diesel generator. *J. Energy Storage* **2023**, *68*, 107621.
17. Abd-El Baset, D.; Rezk, H.; Hamada, M. Fuzzy logic control based energy management strategy for renewable energy system. In Proceedings of the 2020 International Youth Conference on Radio Electronics, Electrical and Power Engineering (REEPE), Moscow, Russia, 12–14 March 2020.
18. Khallouf, K.N.; Laid, Z.; Benbouhenni, H.; et al. Adaptive fuzzy logic control for microgrid-connected hybrid photovoltaic/wind generation systems. *Energy Rep.* **2024**, *12*, 4741–4756.
19. Jasim, A.M.; Jasim, B.H.; Baiceanu, F.C.; et al. Optimized sizing of energy management system for off-grid hybrid solar/wind/battery/biogasifier/diesel microgrid system. *Mathematics* **2023**, *11*, 1248.
20. Mhandu, S.R.; Longe, O.M. Techno-economic analysis of hybrid PV-wind-diesel-battery standalone and grid-connected microgrid for rural electrification in Zimbabwe. In Proceedings of the 2022 IEEE Nigeria 4th International Conference on Disruptive Technologies for Sustainable Development (NIGERCON), Lagos, Nigeria, 17–19 May 2022.
21. Panda, M.; Chankaya, M.; Mohanty, S.; et al. State-of-charge based energy management strategy for hybrid energy storage system in DC microgrid. *IEEE Access* **2025**, *13*, 77353–77364.
22. Rico-Riveros, L.F.; Trujillo-Rodríguez, C.L.; Díaz-Aldana, N.L.; et al. Analysis of a Sustainable Hybrid Microgrid Based on Solar Energy, Biomass, and Storage for Rural Electrification in Isolated Communities. *Appl. Sci.* **2025**, *15*, 10646.
23. Ayele, E.D.; Gonzalez, J.F.; Teeuw, W.B. Enhancing cybersecurity in distributed microgrids: A review of communication protocols and standards. *Sensors* **2024**, *24*, 854.
24. Murugan, G.; Vijayarajan, S. IoT based secured data monitoring system for renewable energy fed micro grid system. *Sustain. Energy Technol. Assess.* **2023**, *57*, 103244.
25. Tang, F.; Guo, Y.; Wei, X.; et al. An intentional controlled islanding strategy considering island frequency stability for power system with wind-power integrated. *Front. Energy Res.* **2023**, *11*, 1247412.

26. Peres, W.; Poubel, R.P.B.; Alipio, R. Probabilistic Load-Shedding Strategy for Frequency Regulation in Microgrids Under Uncertainties. *Symmetry* **2025**, *17*, 1125.
27. Zarma, T.A.; Ali, E.; Galadima, A.A.; et al. Energy Demand Forecasting for Hybrid Microgrid Systems Using Machine Learning Models. *Proc. Eng. Technol. Innov.* **2025**, *29*, 68–83.
28. Aghmadi, A.; Hussein, H.; Mohammed, O.A. Enhancing energy management system for a hybrid wind solar battery based standalone microgrid. In Proceedings of the 2023 IEEE International Conference on Environment and Electrical Engineering and 2023 IEEE Industrial and Commercial Power Systems Europe (EEEIC/I&CPS Europe), Madrid, Spain, 6–9 June 2023.
29. Guanghua, L.; Soomar, A.M.; Shah, S.H.H.; et al. Maximum power point tracking strategies for solar PV systems: A review of current methods and future innovations. *Results Eng.* **2025**, *28*, 107227.
30. León Gómez, J.C.; De León Aldaco, S.E.; Aguayo Alquicira, J. A review of hybrid renewable energy systems: architectures, battery systems, and optimization techniques. *Eng* **2023**, *4*, 1446–1467.